A Study on Bearing Capacity of Steel Sheet Pile with Closed Section at Bottom Supported in Intermediate Layer by Press-In Method

Kazuhide TODA
Researcher, Steel Structures Research Laboratories, Nippon Steel & Sumitomo Metal Corporation, Chiba, Japan
Email: toda.7ay.kazuhide@jp.nssmc.com
Shinji TAENAKA
Chief Researcher, Steel Structures Research Laboratories, Nippon Steel & Sumitomo Metal Corporation, Chiba, Japan
Hidetoshi NISHIOKA
Laboratory Head, Structures Technology Division, Railway Technical Research Institute, Tokyo, Japan
Taisuke SANAGAWA
Assistant Senior Researcher, Structures Technology Division, Railway Technical Research Institute, Tokyo, Japan
Naoyuki KITA
General Manager, Civil Engineering Technology Division, Obayashi Co., Tokyo, Japan
Kosuke MATSUURA
Chief, Civil Engineering Technology Division, Obayashi Co., Tokyo, Japan

ABSTRACT

Conventionally, steel sheet piles have been utilized as earth pressure resisting structures such as riverbank revetments, seawalls, road retaining walls and temporary retaining walls by taking advantage of their excellent horizontal resistance characteristics. In recent years, it is also applied to structures expected for vertical bearing capacity. The "closed-end steel sheet pile", which is expected to exhibit a higher vertical bearing capacity, has been developed by providing a processed and closed cross section of the front end portion of the steel sheet pile. In the Sheet Pile Foundation Method, it has been shown by previous studies that effective reinforcement of substructures can be achieved by using this processed “closed-end steel sheet pile”. However, the bearing capacity characteristics when the “closed-end steel sheet pile” is supported on the intermediate layer is unknown. Therefore, in order to grasp the bearing capacity characteristics when the “closed-end steel sheet pile” was supported on the intermediate layer with SPT N value of about 30, the full-scale load test was carried out. As a result, from the distribution of the axial force and the peripheral resistance, the resistance of the pile-end closed-section zone is sufficiently demonstrated, and it is estimated that the plug of the pile-end closed-section contributes greatly to the bearing capacity development.

Key words: *Steel sheet pile, Bearing capacity, Loading test, Closed-end steel sheet pile, Sheet Pile Foundation*

1. Introduction

Steel sheet piles have been in use over the years as earth pressure resisting structures such as riverbank revetments, seawalls, road retaining walls and temporary retaining walls by taking advantage of their excellent horizontal resistance characteristics. With the growing need for seismic strengthening in recent years, steel sheet piles have also been increasingly used for applications that expect them to bear vertical loads. For example, the PFS Method (Partial Floating Sheet-Pile Method) (**Fig. 1**), in which the isolating effect of steel sheet piles is used, has been proposed as a means of preventing the subsidence of surrounding ground resulting from embankment construction on soft ground. Steel sheet piles have also come into use for seismic strengthening of foundation structures. An example of such steel sheet pile application is the Sheet Pile Foundation Method (**Fig. 2**), in which steel sheet piles and footings are structurally integrated so as to use the steel sheet piles to resist both horizontal and vertical loads. A previous study has shown that an existing foundation structure can be effectively strengthened against seismic loading by use of a steel sheet pile that has a closed section at the toe of the pile (closed-end steel sheet pile), which is designed to achieve large vertical bearing capacity by providing a closed section at the toe of the steel sheet pile.

However, although the vertical bearing capacity of the closed-end steel sheet pile on the bearing layer having an SPT N-value of 50 or more has been verified, the vertical bearing capacity in an intermediate layer is yet to be determined. In addition, bearing capacity characteristics are likely to vary depending on ground conditions. In this study, a series of full-scale loading tests was conducted for a total of four cases tested at two sites to evaluate the bearing capacity of a closed-end steel sheet pile installed into an intermediate layer having an N-value of about 30.

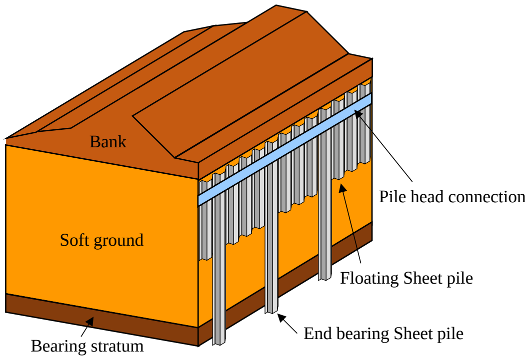

Fig. 1 PFS Method（Partial Floating Sheet-Pile Method）

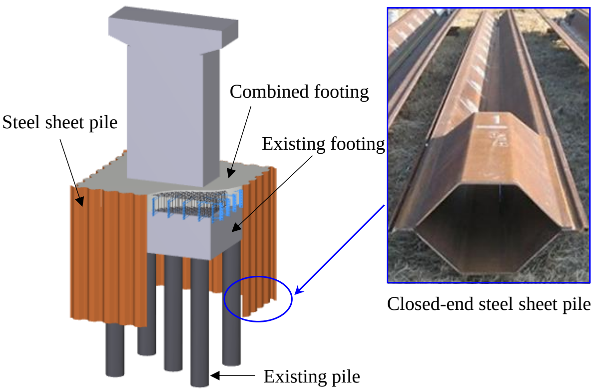

Fig. 2 Sheet Pile Foundation Method

2. Full-Scale test

2.1. Ground condition

The tests were carried out at two places which in Futtsu, Chiba Prefecture, and in Kochi, Kochi Prefecture Japan. The standard penetration test results (SPT-N value) of the test ground are shown in **Fig. 3**. The intermediate layer at the Futtsu site consists of fine sand and has an N-value ranging from about 20 to slightly less than 40. The intermediate layer at the Kochi site consists mainly of sand and gravel and has an N-value of 30 or more at depths of 4 m or more. In the Kochi site, the embedded length in the intermediate layer is longer than $3D_p$ in the closed-section, but in the calculation of the end bearing capacity, only the $3D_p$ section of the closed-section was considered.

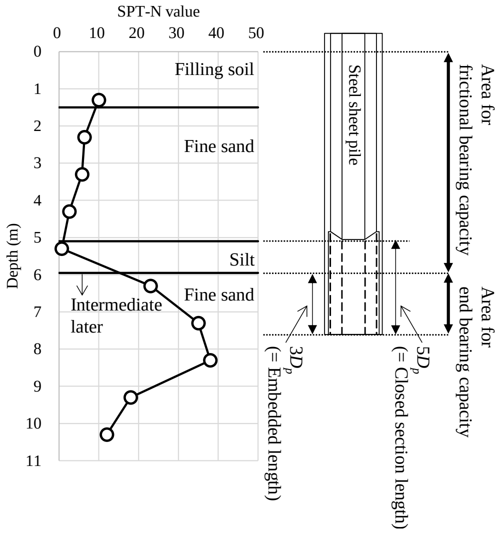

(a) Futtsu (Case1, Case2)

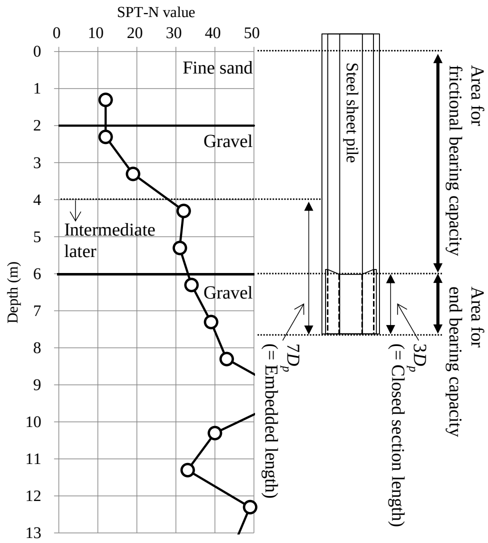

(b) Kochi (Case3, Case4)

Fig. 3 SPT-N value

2.2. Test parameters

2.2.1. Closed-end steel sheet pile

To form the closed section at the toe of the pile, the same type of steel sheet piles as main piles, which has shorter longitudinal length than the main pile, is welded along the interlocks. In full-scale tests, the hat-shape steel sheet piles called 10H and 25H were used. **Table 1** shows these piles.

Table 1. Closed-end steel sheet pile

Pile type	Shape of pile-end closed section (view from the bottom)
10H	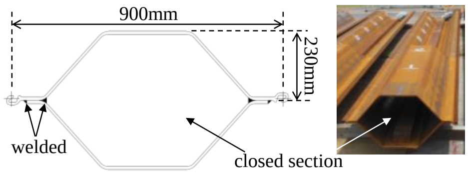
25H	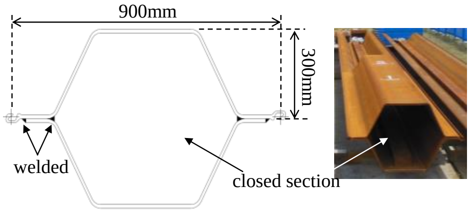

2.2.2. Tests parameters

The test specimens used in the full-scale test are summarized in **Table 2**. The equivalent pile width is represented as D_p (**Fig. 4**). D_p corresponds to the side length of square sections whose area (= A_p) is calculated as the summation of the area surrounded by two steel sheet piles welded together and the plate thickness at the bottom.

According to Nakayama (2012), in the case where a closed-end steel sheet pile is embedded into a bearing layer having an N-value of 50 or more, vertical bearing capacity almost comparable to that of a steel sheet pile that has closed-section construction over the entire length can be achieved if the pile-end closed-section is designed to have a length of 3D_p or more. In accordance with this finding, a pile-end closed-section length of 3D_p was used in Case 3 and Case 4. In Case 1 and Case 2, a pile-end closed-section length of 5D_p was used because the thickness of the layer having an N-value of 30 or more was only 1.5 m (=3D_p).

Table 2. Test specimens for full-scale test

Case	Case1	Case2
Site	Futtsu	
Pile type	10H	25H
Width	0.900m	0.900m
A_p	0.234m^2	0.300m^2
D_p	0.48m	0.55m
Closed-section length	2.40m (= 5D_p)	2.75m (= 5D_p)
Embedded length	1.50m (= 3D_p)	1.50m (= 3D_p)
Case	Case3	Case4
Site	Kochi	
Pile type	10H	10H
Width	900mm	900mm
A_p	0.234m^2	0.234m^2
D_p	0.48m	0.48m
Closed-section length	1.50m (= 3D_p)	1.50m (= 3D_p)
Embedded length	3.50m (= 7D_p)	3.50m (= 7D_p)

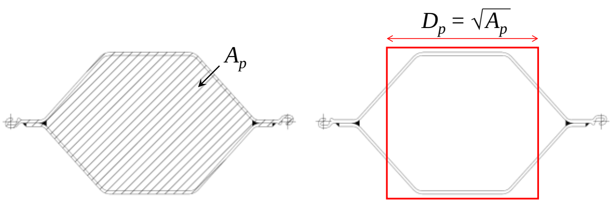

Fig. 4 Equivalent pile width of steel sheet piles

2.3. Full-scale pile installation test

The test specimens were installed into the ground by the press-in method, which is a low-noise, low-vibration pile-installation method that can be used at a site with limited overhead clearance. The water jet was also used to facilitate installation operation. The pile- installation procedures are shown in **Table 3**, and the relationship between press-in force and depth is shown in **Fig. 5**.

In Case 1 and Case 2, water jet pressure was reduced to the idling level (1.1 MPa) at a depth of 1.0 m above the target layer (GL−6.0 m) so as not to disturb the intermediate layer into which the pile was to be embedded (target layer). Then, the pile was pressed in further until it reached the specified depth (GL−7.5 m), and the final press-in force was applied to complete the installation operation.

In Case 3, the original plan was to embed the pile into a bearing layer (GL−12.0 m) having an N-value of 50 or more and stop the pile-end at GL−13.5 m. The pile-end closed-section, therefore, was designed to have a length of $3D_p$. However, the water jet was not able to perform as effectively as expected because consistent water pressure could not be maintained. Installation the pile by a depth of 1.5 m from GL−6.0 m took more than 30 minutes, and further penetration became no longer possible at GL−7.5 m, which was shallower than the target depth. It was decided, therefore, to continue using the water jet at high pressure (15 MPa) until reaching the target depth, and press-in and pull-out operations were repeated. In view of the Case 3 results, the plan for Case 4 was altered so that the pile was embedded into an intermediate layer (GL−6.0 m) and pressed in until it reached a target depth of 7.5 m. Since the steel sheet pile tended to lean toward the water jet equipment during the press-in operation, in Case 4 the water jet equipment was positioned separately at opposite locations as shown in **Fig. 6.** In Case 4, water jetting was used until the target depth was reached as in Case 3. The time required for advancing the pile by a depth of 1.5 m from GL−6.0 m was about 15 minutes, which is half the time required in Case 3.

Table 3. Installation conditions

Case	Depth	Installation conditions
Case1 (10H)	Surface sand layer (GL-0.0～5.0m)	Water pressure (5.0MPa)
	Intermediate layer (GL-5.0～7.5m)	Water pressure (1.1MPa)
	GL-7.5m	Final press-in load (470kN)
Case2 (25H)	Surface sand layer (GL-0.0～5.0m)	Water pressure (5.0MPa)
	Intermediate layer (GL-5.0～7.5m)	Water pressure (1.1MPa)
	GL-7.5m	Final press-in load (490kN)
Case3 Case4 (10H)	Surface sand layer (GL-0.0～2.0m)	Water pressure (3.7MPa)
	Gravel layer (GL-2.0～5.0m)	Water pressure (～14.7MPa)
	Intermediate layer (GL-5.0～7.5m)	Water pressure (1.1MPa)
	GL-7.5m	Water pressure (15.0MPa)

2.4. Full-Scale load test

A full-scale loading test was conducted to evaluate the bearing capacity characteristics of the closed-end steel sheet pile embedded into an intermediate layer without installation it into the bearing layer.

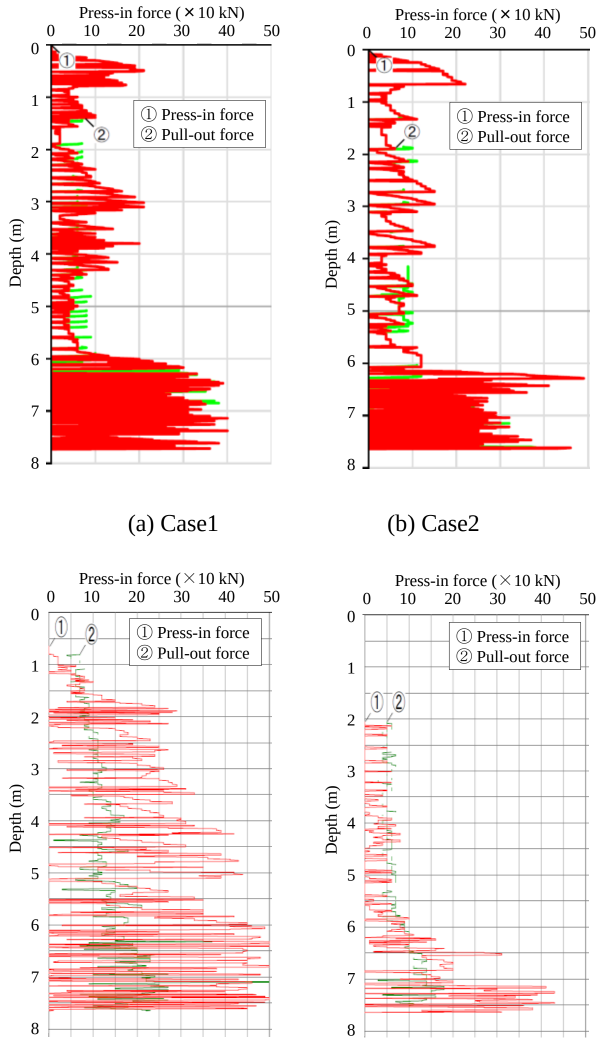

(a) Case1 (b) Case2

(c) Case3 (d) Case4

Fig. 5 Relationship between press-in force and depth

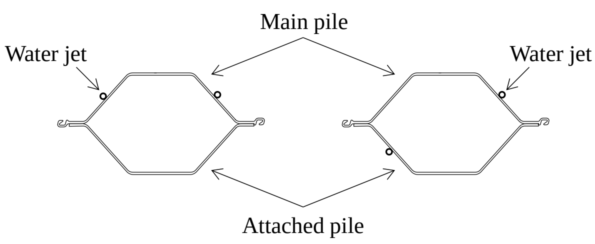

(a) Case1, Case2, Case3 (b) Case4

Fig. 6 Arrangement of water jet

2.4.1. Test procedures

The full-scale loading test consisted of a rapid loading test and a static loading test. Both load tests were carried out when 33 to 43 days had passed since the completion of the installation tests. The test method is based on the standard method provided by the Japanese Geotechnical Society (2002).

At the Futtsu site, the rapid loading test was conducted. In the test, a 260-kN-weight was dropped from 14 different heights ranging from 21 cm to 281 cm for the type 10H piles and from 12 different heights ranging from 25 cm to 285 cm for the type 25H pile (last three drops from the same height). For both types of piles, the arrival at the 10%-of-pile-diameter subsidence level ($0.1D_p$) was confirmed at the end of the loading test.

At the Kochi site, the static loading test was conducted. Loading was carried out as a seven-cycle process, and the maximum loads applied during the seven cycles were 200 kN, 400 kN, 600 kN, 800 kN, 1,300 kN, 2,000 kN and 2,100 kN. It was made a rule to increase the applied load at a rate of 50 kN/min and decrease it at a rate of 100 kN/min. Holding time for each loading step was as follows: a constant period no less than 30 minutes of new loading steps, a constant period no less than 2 minutes of unloading or reloading steps and a constant period no less than 15 minutes of unloading to zero load before moving on to the next loading stage. In Case 3, the 10%-of-pile-diameter subsidence ($0.1D_p$) was reached during the fifth cycle, and in Case 4, $0.1D_p$ was reached during the seventh cycle to end the test. The maximum load reached in the test was 2,000 kN in Case 3 and 2,100 kN in Case 4.

2.4.2. Loading test results

2.4.2.1. Comparison with estimated bearing capacity

Railway Technical Research Institute (2014) proposed formulas for calculating the bearing capacity of a closed-end steel sheet pile. The proposed formulas are based on various full-scale loading test results. The bearing capacity is defined as the resistance force of a pile when the pile-end displacement has reached $0.1D_p$ against vertical load. The proposed formulas are as follows:

・End bearing capacity

$q_{tk} = \beta_{wjq} \times 105\,N$ (≦4000) (sand)

(≦6000) (gravel) (1)

・Frictional resistance

$r_{fk} = \beta_{wjr} \times 3\,N$ (≦40) (sand or gravel) (2)

where q_{tk} is intensity of the end bearing capacity (kN/m^2); r_{fk}, intensity of the frictional resistance (kN/m^2); β_{wjq}, β_{wjr}, reduction due to water jet (= 1/3); and N, SPT N-value at the tip of the steel sheet pile.

Also, in the calculation of end bearing capacity, A_p shown in **Fig. 4** is defined as the tip closure area.

Fig. 7 shows the rapid loading test results in Case 1 and Case 2, along with the maximum unloading point resistance results obtained by the unloading point method (Japanese Geotechnical Society (2002)). **Table 4** shows the pile-head and pile-end bearing capacities at $0.1D_p$. In the test specimen used in Case 1 shown in **Fig. 7 (a)**, a measured unloading point resistance of 722.9 kN was obtained at $0.1D_p$ (= 48 mm), and after the tendency of resistance to increase was observed, a maximum unloading point resistance of 920.0 kN was observed during the 12th cycle. In Case 2 shown in **Fig. 7 (b)**, a maximum unloading point resistance of 1,028.6 kN was observed during the 10th cycle. After that, resistance showed a tendency to decrease, and then 948.4 kN was observed at $0.1D_p$ (= 55 mm). As shown in **Table 4**, the bearing capacity at $0.1D_p$ was about 15 times and 20 times the final press-in load in Case 1 and Case 2, respectively.

From the strain gauge installed in each test

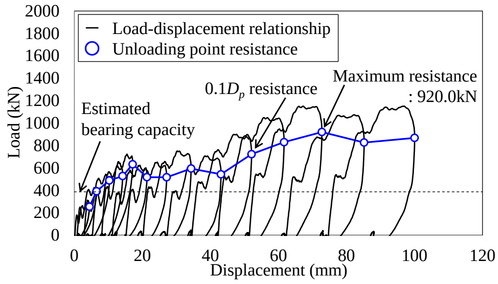

(a) Case1

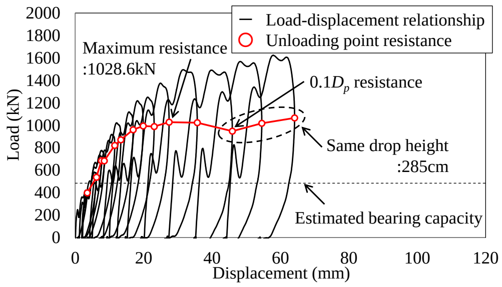

(b) Case2

Fig. 7 Relationship between vertical load and displacement specimen, a graph showing the depth distribution of axial force was prepared, and the results corresponding to $0.1D_p$ and the maximum resisting force were compared. And, the axial force of the pile-head was taken as the unloading point resistance calculated from the strain gauge at the part protruding from the ground surface. In the evaluation of end bearing capacity, as shown in **Fig. 3**, the axial force at the section for $3D_p$ above the pile-end was taken as the tip resistance. In the axial force distribution graph for Case 1 shown in **Fig. 8 (a),** resistance was seen to increase from the $0.1D_p$ level to the maximum unloading point resistance level. The ratio between end bearing capacity and pile-head resistance, however, did not change significantly, ranging from about 83% to 87%. In Case 2, as shown in **Fig. 8 (b)**, the end bearing capacity did not change, indicating that the tendency of resistance to decrease from the maximum unloading point resistance level to the $0.1D_p$ level shown in **Fig. 7 (b)** is due to changes in frictional resistance. In both cases, it can be clearly seen that resistance in the intermediate layer into which the pile-end was embedded increased sharply. From this, it can be inferred that although the pile was supported by an intermediate layer, resisting force occurred mainly in this region so that the closed-end steel sheet pile effectively contributes to bearing capacity.

Fig. 9 shows the static load test results in Case 3 and Case 4. **Fig. 10** shows the depth distributions of axial force and frictional resistance. From **Fig. 9**, in Case 3, first limit resistance is estimated to be 500 to 800 kN, and a measured second limit resistance of 1,178 kN was recorded at $0.1D_p$ (= 48 mm). In Case 4, first limit resistance was estimated to be 1,000 kN, and a measured second limit resistance of 1,812 kN was recorded at $0.1D_p$ (= 48 mm), which is greater than in Case 3 by a factor of about 1.5. It was also confirmed that in the sand and gravel ground, too, the estimated level of bearing capacity can be achieved in a bearing layer that has an SPT N-value of 50 or more. In all cases, resistance tended to continue to increase after $0.1D_p$ was reached.

2.4.2.2. Bearing capacity depending on shape of sheet piles

As shown in **Table 4**, the end bearing capacity in the 25H case (Case 2) was greater than that in the 10H case

Table 4. Loading test results

Case		$0.1D_p$ resistance	
Case1 (10H)	Bearing capacity	722.9	kN
	End bearing capacity	630.2	kN
	Ratio of End bearing capacity to Bearing capacity	87.2	%
	Bearing capacity / Final press-in force	15.4	
Case2 (25H)	Bearing capacity	948.4	kN
	End bearing capacity	775.5	kN
	Ratio of End bearing capacity to Bearing capacity	81.8	%
	Bearing capacity / Final press-in force	19.4	
Case3 (10H)	Bearing capacity	1178	kN
	End bearing capacity	385	kN
	Ratio of End bearing capacity to Bearing capacity	32.7	%
Case4 (10H)	Bearing capacity	1812	kN
	End bearing capacity	859	kN
	Ratio of End bearing capacity to Bearing capacity	47.4	%

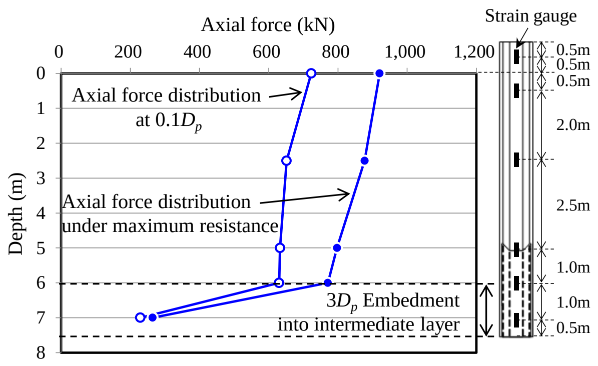

(a) Case1

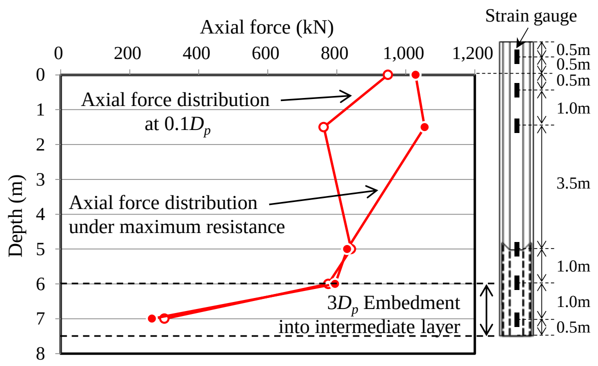

(b) Case2

Fig. 8 Relationship between axial force and depth

(Case 1) by a factor of about 1.2, which was similar to the pile-end closed-section area ratio (A_p). Frictional resistance was greater than in the 10H case (Case 1) by a factor of about 1.5, which was greater than the cross-sectional perimeter ratio of 1.1.

2.4.2.3. End bearing capacity depending on length of closed section

In the full-scale test, in which the pile was embedded into an intermediary layer without installing it into the bearing layer, the length of the pile-end closed-section was varied depending on ground conditions. As can be seen from **Fig. 7** and **Fig. 9**, the estimated bearing capacity can be achieved by using 5D_p for a sand layer and 3D_p for a sand and gravel layer. Therefore, this estimation formula is on the safety side (lower side). And from **Fig. 8**, the increase in axial force is small within the range of 3D_p to 5D_p in the pile-end closed-section, and does not contribute much to the pile tip plugging. Whether 3D_p, which is similar to the value reported in a previous study focusing on a bearing layer having an N-value of 50 or more, may be applied to a sand layer needs to be determined by checking on bearing capacity characteristics through further load testing.

2.4.2.4. Bearing capacity depending on arrangement of water jet

In Case 3, in which a pile installation challenge was encountered, the frictional resistance of the embedded part of the pile was smaller than at GL−6.0 m or shallower depths as shown in **Fig. 10 (a)**, and, as shown in **Table 4**, the ratio of end bearing capacity to bearing capacity decreased to about 30%. In contrast, in Case 4, in which water jet equipment was positioned at opposite locations to facilitate pile installation work, significant frictional force was achieved by the pile-end closed-section zone as shown in **Fig. 10 (b)** so that its ratio of end bearing capacity to bearing capacity was roughly 50%. Also, as shown in **Table 4**, there is a significant difference in end bearing capacity: the end bearing capacity in Case 4 is greater than that in Case 3 by a factor of greater than 2. The reason for this is thought to be that because the water jet equipment was installed at opposite locations in Case 4, the leaning of the steel sheet pile was reduced. This resulted in reduced use of water jetting, a reduced number of repetitions of press-in and pull-out operations, and reduced ground disturbance mainly in the pile-end zone.

2.4.2.5. Comparison with the loading test results of previous

Fig. 11 shows the relationship with the loading test results obtained from steel sheet piles embedded into bearing layers having an SPT N-value of 50 or more reported by the Railway Technical Research Institute

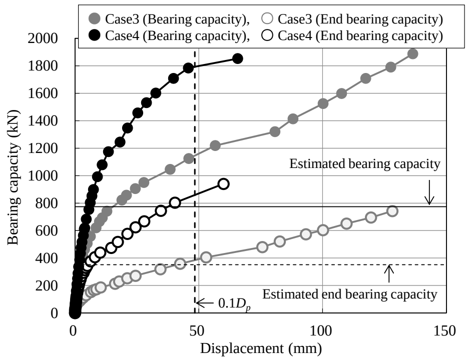

Fig. 9 Relationship between bearing capacity and displacement

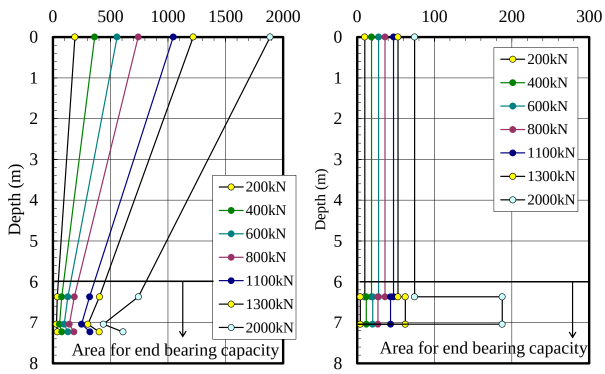

(a) Case3

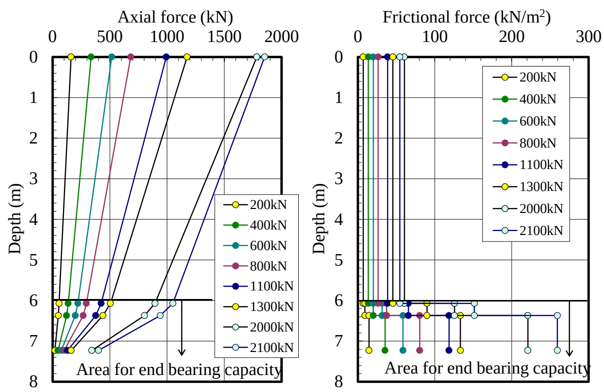

(b) Case4

Fig. 10 Depth distribution of axial force and frictional force

(2014). As can be seen from **Fig. 11**, the relationship with the expected bearing capacity in the cases where the steel sheet pile is embedded into an intermediate layer having an N-value of around 30 is similar to the relationship in the cases where the steel sheet pile is embedded into a bearing layer having an N-value of 50 or more.

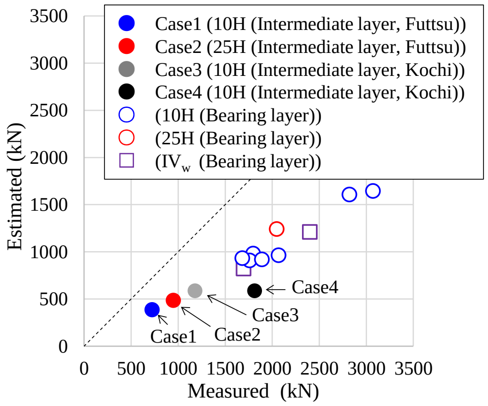

Fig. 11 Comparison with the past of loading test results

3. Concluding remarks

To evaluate bearing capacity characteristics of a closed-end steel sheet pile embedded into an intermediate layer, a series of full-scale pile-installation and loading tests was conducted at two sites.

Closed-end steel sheet piles were installed into the ground by the press-in method used in conjunction with water jetting. At the sandy soil site, water jet pressure was reduced to the idling level at a depth 1 m above the intermediate layer before embedding the pile into the intermediate layer. At the sand and gravel site, water jetting was used until the pile reached the target depth. Installing water jet equipment at opposite locations around the pile reduced press-in resistance and the time required for reaching the embedment layer.

Axial force and frictional resistance distributions confirmed that even in the cases where the pile was embedded into an intermediate layer without installation it into the bearing layer, the embedded pile-end closed-section zone served as a major contributor to resistance so that the closed-end steel sheet pile effectively contributed to bearing capacity. Even in the cases where the pile was embedded into an intermediate layer without installation it into the bearing layer, the expected level of bearing capacity was achieved as in the case where the pile was embedded into the bearing layer having an SPT N-value of 50 or more, confirming that the achieved bearing capacity is comparable to the expected bearing capacity.

Length requirements for the pile-end closed-section vary depending on the ground conditions involving the target layer, and the required lengths for a sand layer and a sand and gravel layer are $5D_p$ and $3D_p$, respectively. In cases where water jetting is used to assist in pile installation, it is advisable to reduce water pressure to the idling level at a depth 1 m above an intermediate layer so as to minimize the disturbance of the target layer. In cases where water pressure is difficult to maintain because of ground conditions, pile installation resistance increases if the steel sheet pile being installed leans sideways. In such cases, ground disturbance around the pile-end during embedment operation may affect bearing capacity development. It is therefore necessary to take some corrective measures such as positioning water jet equipment at opposite locations.

References

Society for Study Group of PFS Method. 2005. PFS Method technical data.

Railway Technical Research Institute, Obayashi Corporation, Nippon Steel & Sumitomo Metal Corporation. 2014. Design and construction manual for sheet pile foundations applied to railway structures (draft), 3rd ed. (in Japanese)

Nakayama, H., Koda, M., Nishioka, H., Sanagawa, T., Harata, N., Kato, A., Toda, K. 2012. Static load test on vertical bearing capacity of steel sheet piles with closed section, 9th Int. Conf. on Testing and Design Methods for Deep Foundations.

Japanese Geotechnical Society. 2002. Standard for vertical load tests of piles.

Railway Technical Research Institute. 2012. Design Standard for Railway Structures (Foundation Structures), Maruzen. (in Japanese)

Toda, K., Nishioka, H., Sanagawa, T., Taenaka, S., Otsushi, K., Kita, N., Matsuura, K. 2016. Evaluation of bearing capacity of steel sheet pile with closed section at bottom supported in intermediate layer based on loading test data, 60th Japanese geotechnical engineering symposium, pp. 255-260.